

## **Supporting Information**

### **Real-Time Surface-Enhanced Raman Scattering-Based Live Cell Monitoring for the Changes of Mitochondrial Membrane Potential**

Ji Hye Lee, Hyeon Jeong Shin, Yong Duk Kim, and Dong-Kwon Lim\*

KU-KIST Graduate School of Converging Science and Technology, Korea University, 145 Anam-ro, Seongbuk-gu, Seoul, South Korea. E-mail: [dklim@korea.ac.kr](mailto:dklim@korea.ac.kr).

\*Correspondence to Prof. Dong-Kwon Lim, [dklim@korea.ac.kr](mailto:dklim@korea.ac.kr).

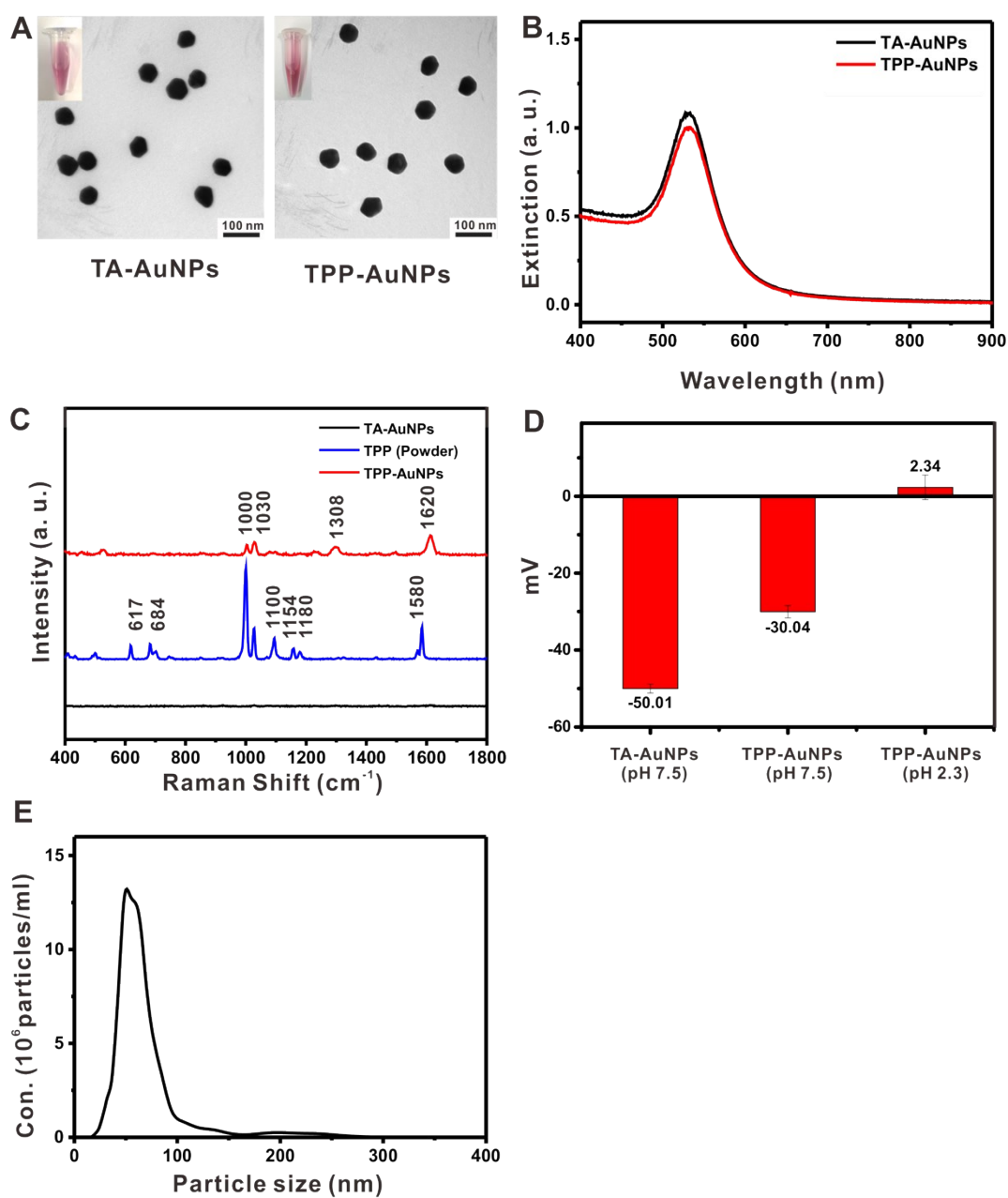


**Figure S1.** (A) TEM images [TA-AuNP, TPP-AuNP solution (inset)], (B) UV-visible spectrum, (C) Raman spectra, and (D) zeta potential analysis of TA-AuNPs and TPP-AuNPs, (E) hydrodynamic radius of TPP-AuNPs.

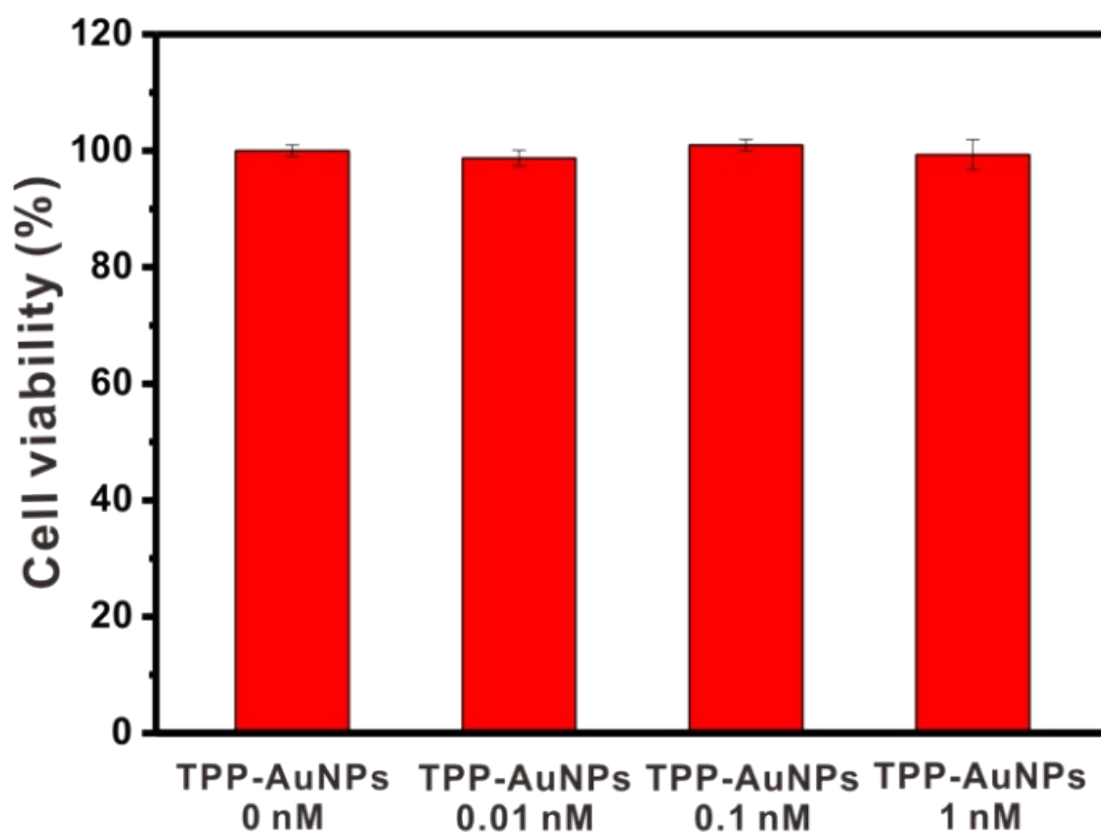


**Figure S2.** Cell viability results of control (0 nM) and TPP-AuNPs in RASFs at different concentrations (0.01 nM, 0.1 nM, and 1.0 nM) for 3 h (N = 4).

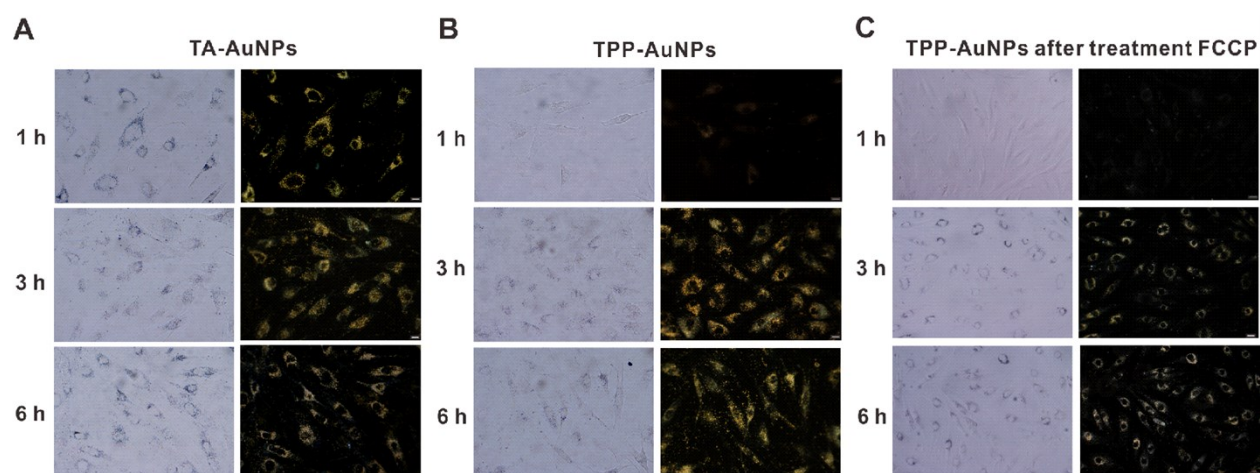


**Figure S3.** (A) Intracellular distribution of TA-AuNPs in RASFs observed by bright-field and dark-field microscopy after 1 h, 3 h, and 6 h. (B) Intracellular distribution of TPP-AuNPs in RASFs observed by bright-field and dark-field microscopy after 1 h, 3 h, and 6 h. (The initial concentration in cell culture media was 0.1 nM). (C) Intracellular distribution of TPP-AuNPs in RASFs 1 h, 3 h, and 6 h after treatment with FCCP (20  $\mu$ M, 10 min) using bright-field and dark-field microscopy. (The initial concentration in cell culture media was 0.1 nM). Scale bar = 50  $\mu$ m.

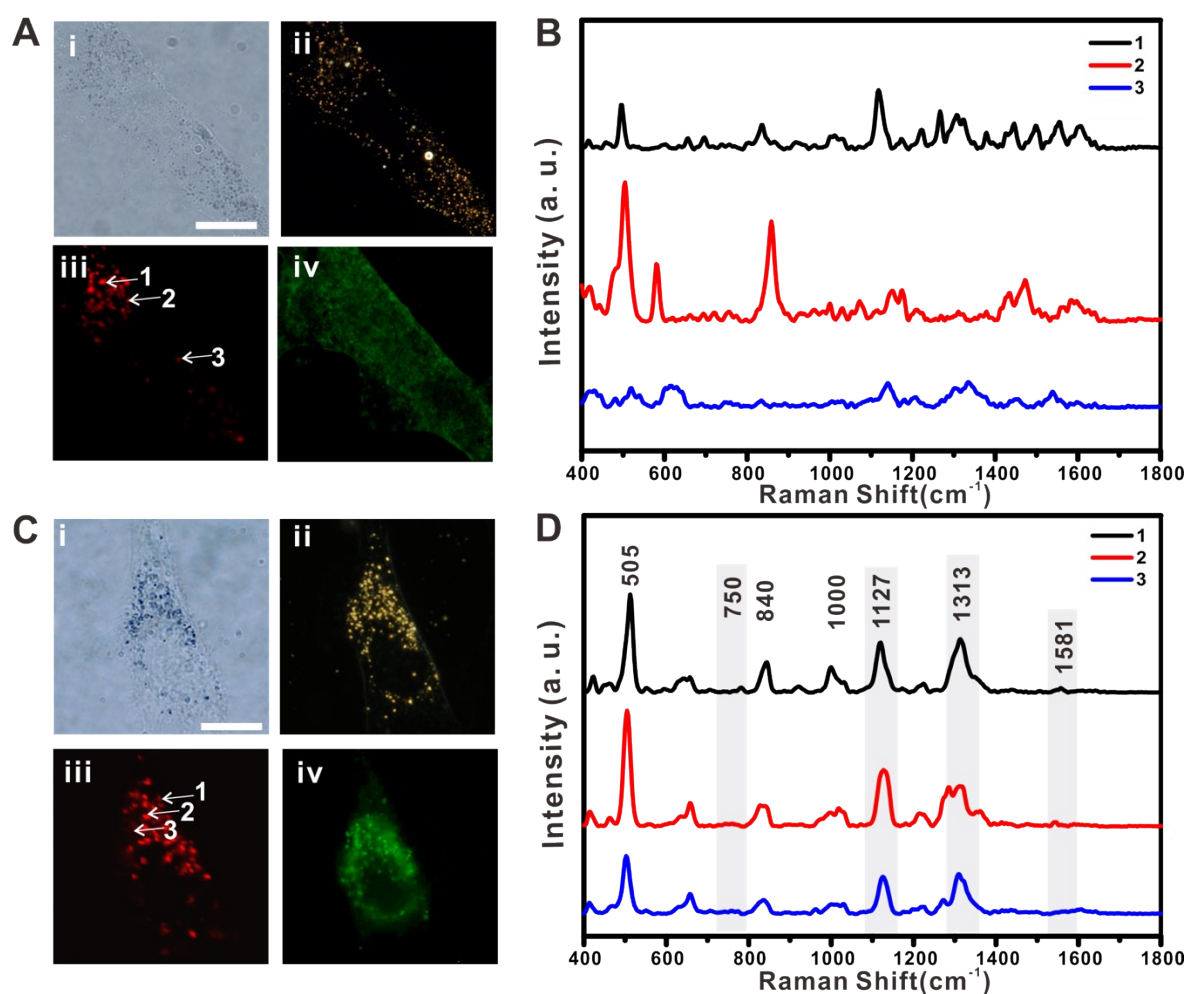


**Figure S4.** (A) Intracellular distribution of TA-AuNPs in rheumatoid arthritis synovial fibroblasts (RASFs) observed with bright field microscopy (i), dark field microscopy (ii), Raman mapping (iii), and fluorescence images (iv) stained with mito-tracker. (B) Raman spectra obtained from inside cells (A-iii, points 1, 2, and 3). (C) Intracellular distribution of TPP-AuNPs in rheumatoid arthritis synovial fibroblasts observed with bright field microscopy (i), dark field microscopy (ii), Raman mapping (iii) and fluorescence images (iv) stained with mito-tracker. (D) Raman spectra obtained from inside cells (C-iii, points 1, 2, and 3). Raman signals at 750, 1127, 1313, and 1581  $\text{cm}^{-1}$  are assigned to the vibration mode of cytochrome c. (Scale bars = 20  $\mu\text{m}$ ).

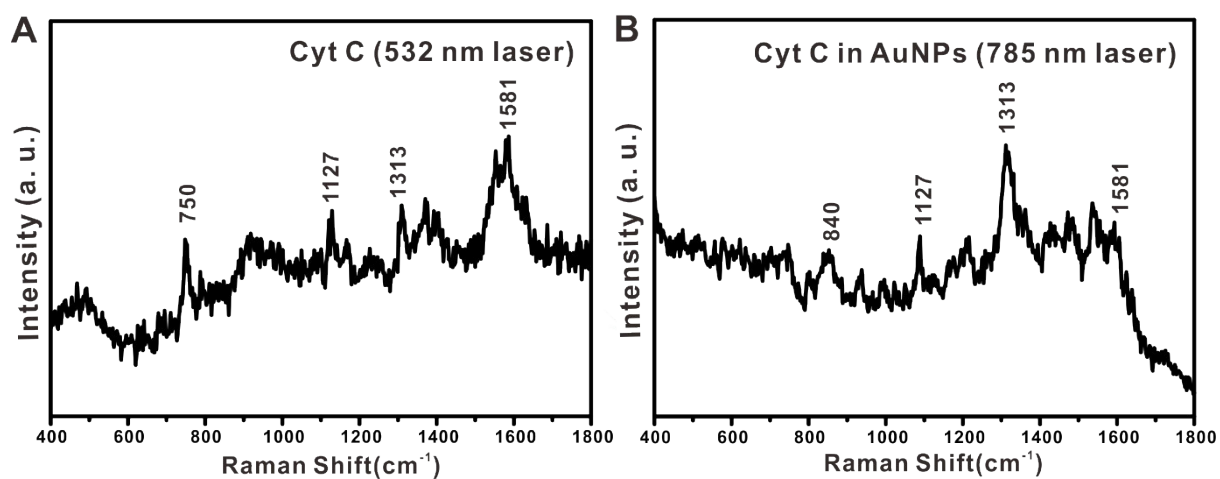


**Figure S5.** (A) Raman spectra of Cyt C obtained with 532 nm laser excitation, (B) Raman spectra of Cyt C obtained with 785 nm laser excitation.

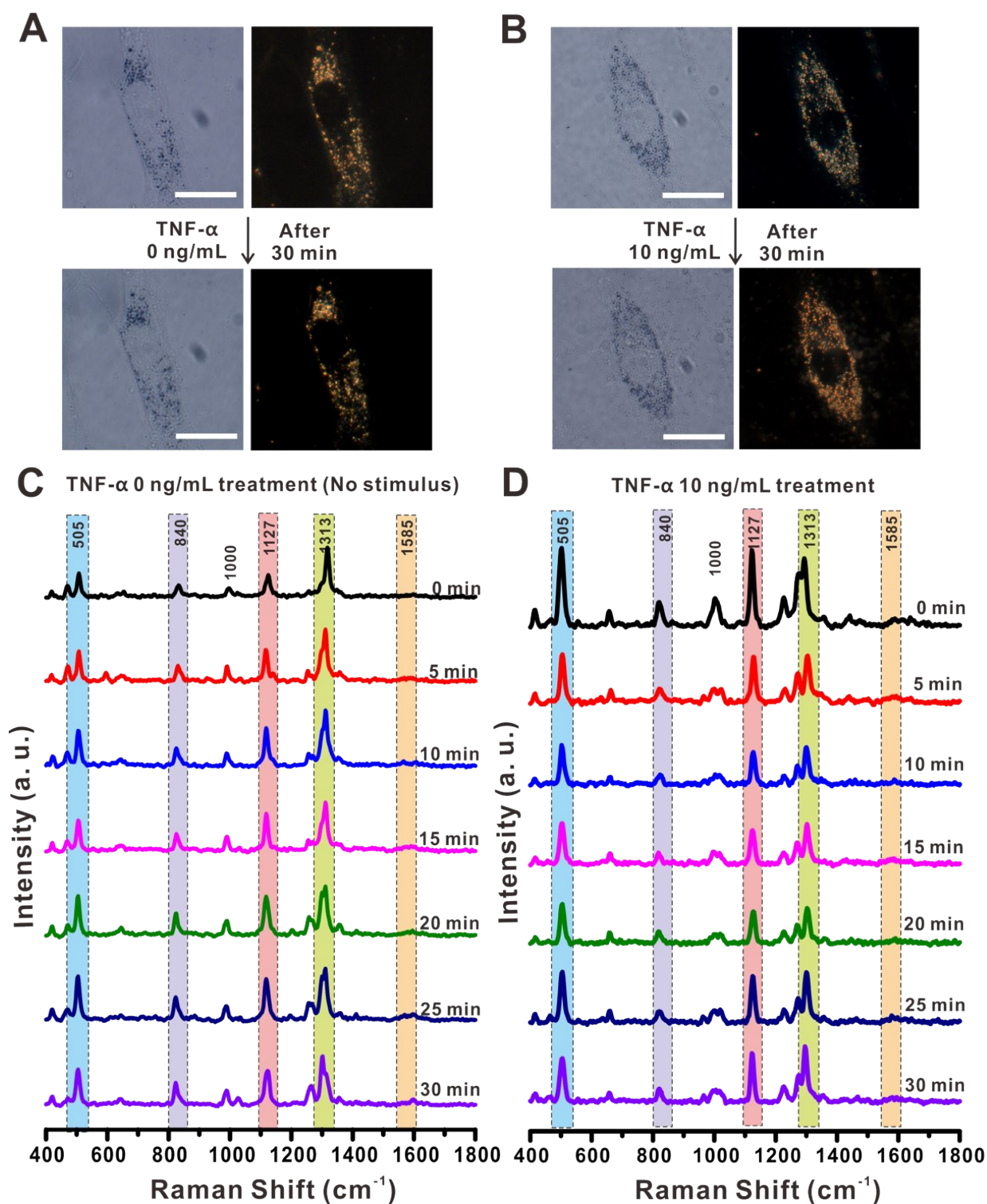


**Figure S6.** Bright-field and dark-field images before (A) and (B) after addition of 10 ng/mL TNF- $\alpha$  in RASFs. Time-dependent changes in Raman spectra from a single cell with (C) no stimulus and after addition of (D) 10 ng/mL TNF- $\alpha$ . Scale bar = 20  $\mu\text{m}$ .



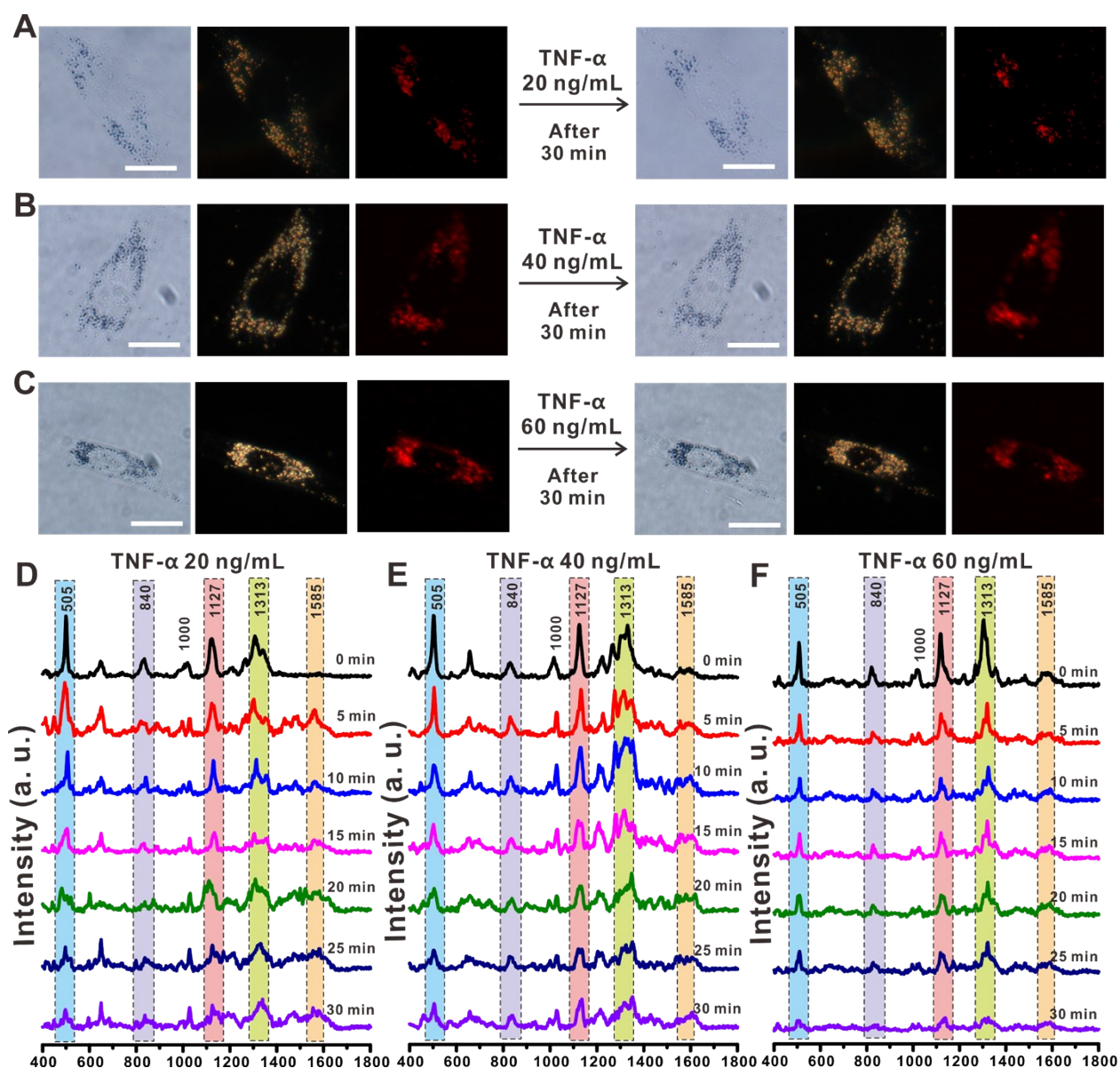


**Figure S7.** Bright-field, dark-field, and Raman images before and after addition of (A) 20 ng/mL, (B) 40 ng/mL, or (C) 60 ng/mL TNF-  $\alpha$  in RASFs. Time-dependent changes in Raman spectra from a single cell after the addition of (D) 20 ng/mL, (E) 40 ng/mL, or (F) 60 ng/mL TNF-  $\alpha$ . Scale bar = 20  $\mu$ m.



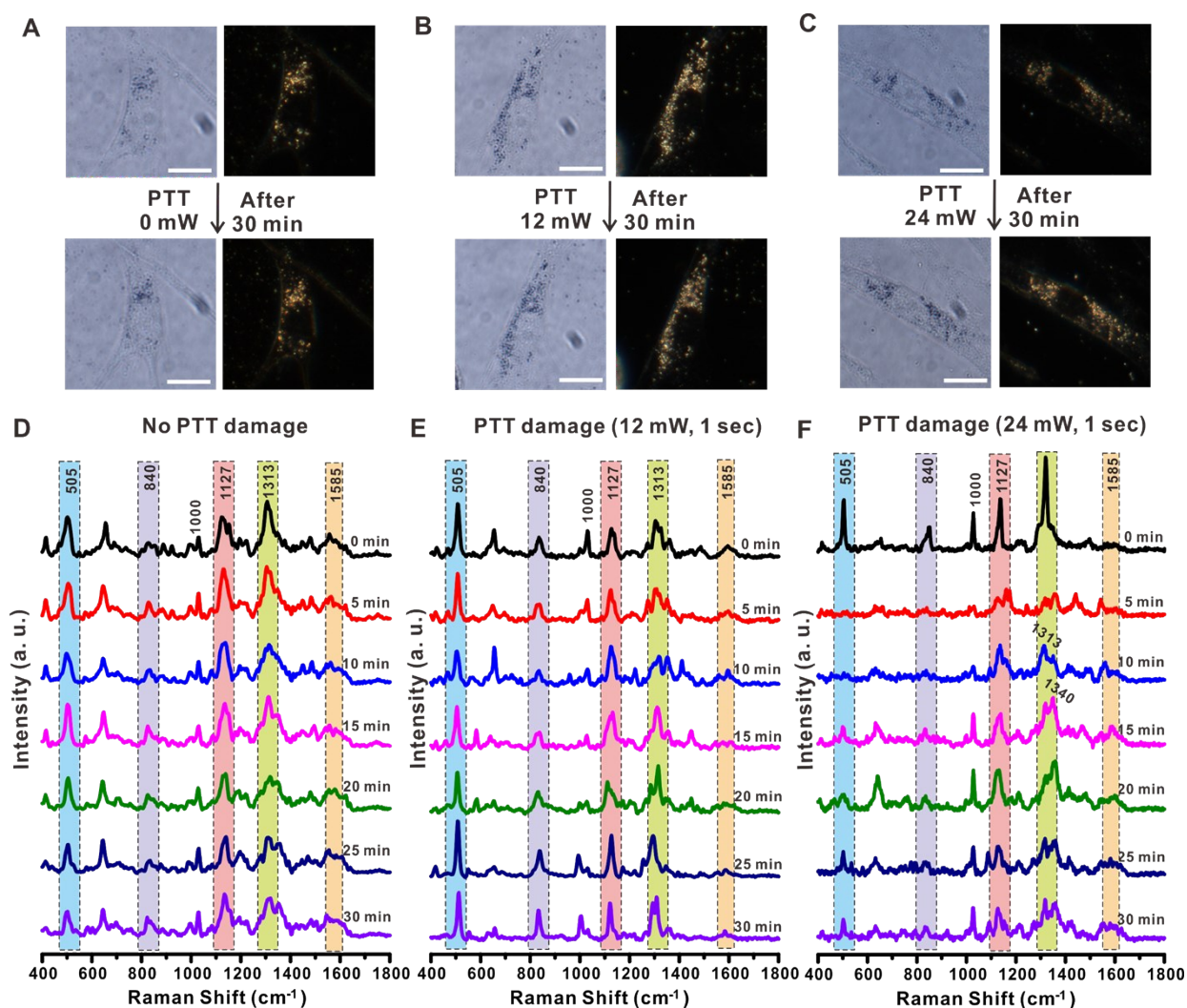


**Figure S8.** Bright-field and dark-field images before (A) and (B) after photothermal damage applied using a focused a laser of 12 mW (785 nm) or (C) 24 mW (785 nm) for 1 s. Scale bar = 20  $\mu\text{m}$ . Time-dependent changes in Raman spectra from a single cell with (D) no photothermal damage, (E) with photothermal damage applied using a focused a laser of 12 mW (785 nm) for 1 s, or (F) with photothermal damage applied using a focused a laser of 24 mW (785 nm) for 1 s.

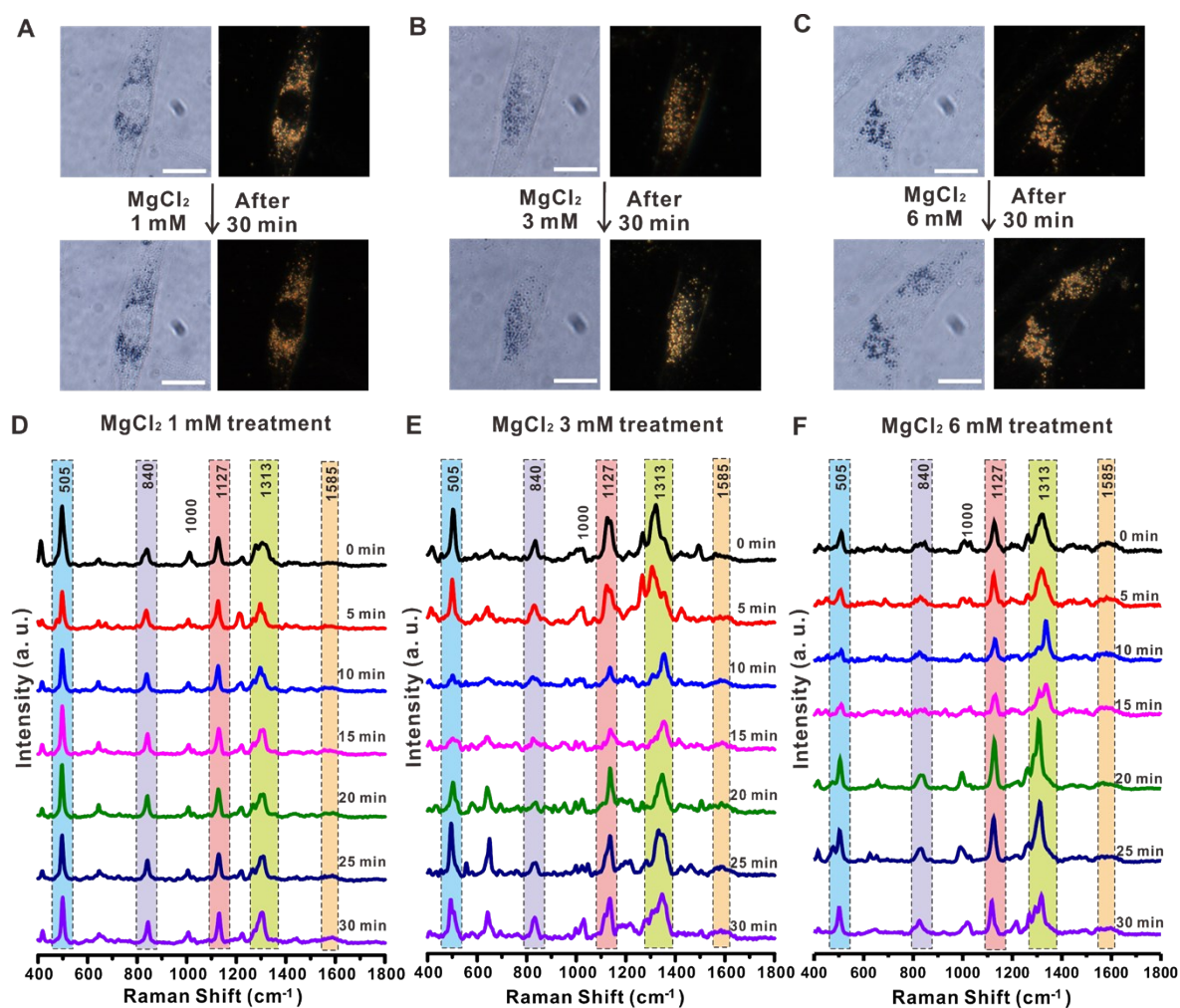


**Figure S9.** Bright-field and dark-field images before and after the addition of (A)  $\text{MgCl}_2$  (1 mM), (B) 3 mM  $\text{MgCl}_2$ , or (C) 6 mM  $\text{MgCl}_2$  in RASFs. Scale bar = 20  $\mu\text{m}$ . Time-dependent changes in Raman spectra from a single cell after the addition of (D) 1 mM  $\text{MgCl}_2$ , (E) 3 mM  $\text{MgCl}_2$ , or (F) 6 mM  $\text{MgCl}_2$ .

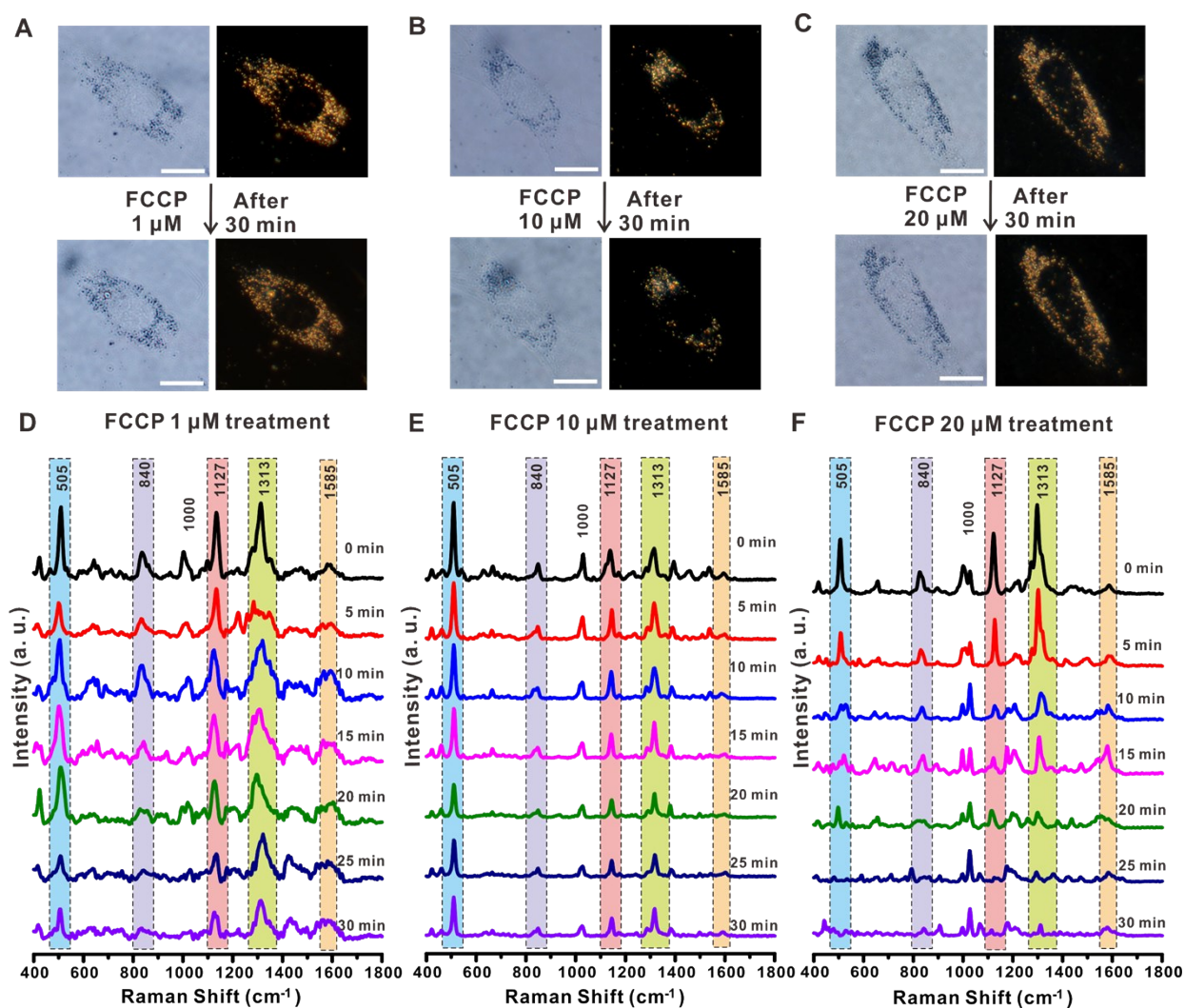


**Figure S10.** Bright-field and dark-field images before and after the addition of (A) 1  $\mu\text{M}$ , (B) 10  $\mu\text{M}$ , or (C) 20  $\mu\text{M}$  FCCP in RASFs (scale bar = 20  $\mu\text{m}$ ). Time-dependent changes in Raman spectra from a single cell after the addition of (D) 1  $\mu\text{M}$ , (E) 10  $\mu\text{M}$ , or (F) 20  $\mu\text{M}$  FCCP.



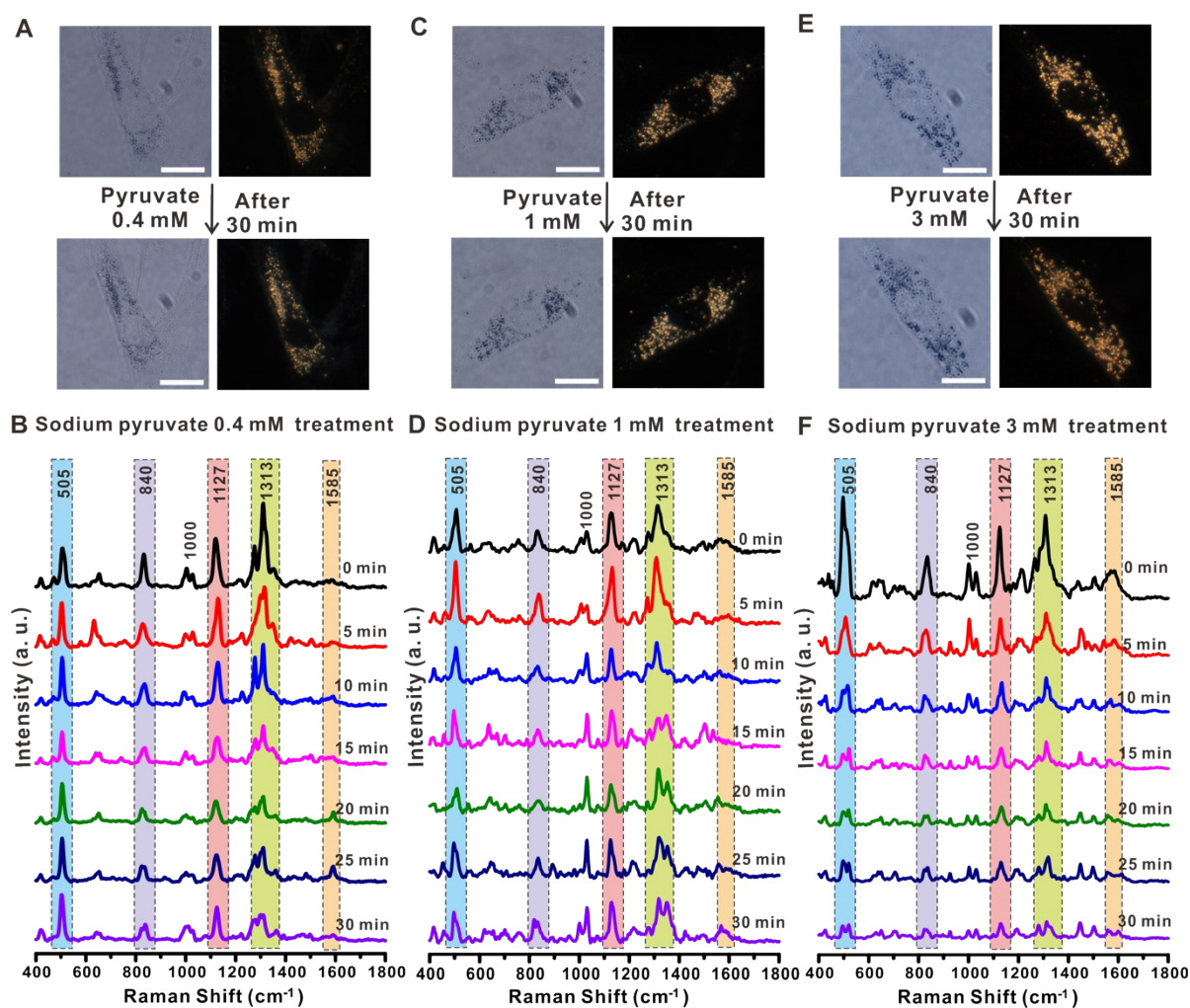


**Figure S11.** Bright-field and dark-field images before and after the addition of (A) 0.4 mM, (B) 1 mM, or (C) 3 mM sodium pyruvate in RASFs (scale bar = 20  $\mu$ m). Time-dependent changes in Raman spectra from a single cell after the addition of (D) 0.4 mM, (E) 1 mM, or (F) 3 mM sodium pyruvate.

